Influence of the thermoelectric effect on the Rayleigh-Bénard instability inside a magnetic field

N. Kurenkova, E. Zienicke, and A. Thess
Department of Mechanical Engineering, Ilmenau University of Technology P.O. Box 100565, 98684 Ilmenau, Germany
(Received 7 September 2000; published 30 August 2001)

We investigate the influence of thermoelectric effect on the onset of thermal instability in the Rayleigh-Bénard system with vertical magnetic field. An electrically conducting fluid is confined in an infinite horizontal layer between thick thermally and electrically conducting walls. A horizontal temperature variation resulting from convective instability leads to horizontal temperature gradients along the liquid-solid interface acting as a source of thermoelectric currents. Through interaction with the applied magnetic field, the Lorentz force is created modifying the instability. We find that the critical Rayleigh number for onset of convection is not changed by the thermoelectric effect. However, the thermal gradient on the liquid-solid boundary leads to a change of the shape of the unstable mode creating helical flow in the evolving convection rolls because of the Lorentz force parallel to their axis. The created kinetic helicity depends linearly on the dimensionless parameter K_{TE} characterizing the strength of the thermoelectric effect.

DOI: 10.1103/PhysRevE.64.036307 PACS number(s): 47.20.Bp, 72.15.Jf, 47.65.+a

I. INTRODUCTION

The influence of an uniform magnetic field on the Rayleigh-Bénard instability with an electrically conducting fluid has already been the subject of intensive study, experimentally as well as theoretically (see, for example, Nakagawa [1–3] for experimental work and Chandrasekhar [4] and Moreau [5] for a review of the theoretical background). The aspect that we consider in our paper is the action of thermoelectric effect at the interface between the fluid and the horizontal walls, which confine the fluid and are also assumed to be electrically conducting. Considering thick walls there will be horizontal temperature gradients at the interface leading to thermoelectric currents creating the Lorentz force in the fluid by interaction with the magnetic field.

Our motivation to study the thermoelectric effect in magnetoconvection is twofold. On the one hand, the understanding of the interaction between electrically conducting fluids and Lorentz force of thermoelectric origin presents a challenge to fundamental fluid dynamics. Although Shercliff [6] has formulated the theoretical framework of thermoelectric magnetohydrodynamics (TEMHD) as early as 1979, there are still very few TEMHD prototype problems that have been well understood. Rayleigh-Bénard convection is well suited to advance our understanding of TEMHD convection because it is conceptually simple and amenable to analytic treatment.

On the other hand, interactions between thermoelectric currents and an external magnetic field in liquid metals occur in a wide range of material processing operations, where solidification processes of metals, alloys or semiconductors have to be optimized in industrial processes. For instance, the thermoelectric effect has attracted attention in the last years from authors considering continuous casting [7], dendritic growth of alloys [8–10], and semiconductor crystal growth [11]. Convection as a key mechanism of heat transport inside the liquid phase has a large influence on the solidification process, especially on the development of the solid-liquid interface. A certain kind of melt convection can be positive or negative for the resulting crystal, normally one has to carry out an optimization between different effects to get a crystal with the wanted properties (homogeneity, purity, etc.). For example, in crystal growth of semiconductors a positive effect of convection can be the homogeneous distribution of dopants, or the suppression of segregation, if one considers the solidification of an alloy (see, for example [12]). Stationary magnetic fields normally have the tendency to suppress convection (for example, convection originating from bouyancy effects). For the use of stationary magnetic fields in crystal growth processes see [13]. Including also the thermoelectric effect one has two effects partly working against each other: convection driven by the Lorentz force because of thermoelectric currents and the braking effect of the magnetic field on bouyancy convection. With the strength and the shape of the external magnetic field one has the possibility to vary the ratios between the strength of the thermoelectric force, the MHD influence of the external magnetic field on convection and bouyancy forces.

Investigating the stability problem in the Rayleigh-Bénard problem with external magnetic field and thermoelectric effect we hope to contribute to gain the physical understanding of TEMHD that is necessary to use magnetic fields for the control of solidification processes in electrically conducting melts in an optimal way.

The paper is organized as follows. In the next section, i.e., Sec. II, we give the formulation of the problem, the governing equations, and the boundary conditions. We explain the way how the thermoelectric effect is taken into account. Using linear stability analysis the equations for the determination of the unstable modes and the critical Rayleigh number are derived. The results of the numerical computations are presented in Sec. III. We demonstrate the influence of the magnetic field and the conducting walls on the stability state of the given Rayleigh-Bénard system. The numerical solution of the velocity, temperature, vorticity, and current density functions is found. Also in Sec. III the action of the thermoelectric effect is quantitatively analyzed. The angle γ of the convection rolls deviation is determined and presented as a function of the parameter K_{TE} characterizing the strength of the thermoelectric effect. The influence of the

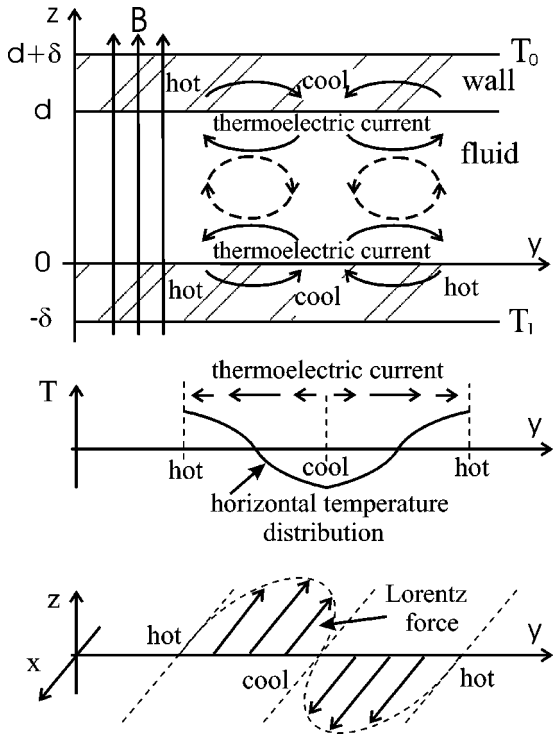

FIG. 1. Rayleigh-Bénard convection between thick walls (convection rolls, dashed line). Hot and cold areas on the interface between solid and fluid induce thermoelectric currents. These then create the Lorentz force by interaction with the homogeneous magnetic field.

thermoelectric effect is also expressed in terms of the relative kinetic helicity. Section. IV contains conclusions and calculation of the angle γ for the Al-Li pair as a solid-liquid system.

II. LINEAR STABILITY ANALYSIS

We consider an electrically conducting fluid in a horizontal layer of thickness d, restricted by electrically conducting walls of thickness δ from above and below. The layer extends infinitely in the horizontal x- and y-directions (see Fig. 1). Fixed values for the temperature are maintained at the bottom of the lower wall, where $T(z=-\delta)=T_1$, and at the top of upper wall, where $T(z=d+\delta)=T_0<T_1$. $\tilde{\beta}=(T_1-T_0)/(d+2\delta)$ is the corresponding steady adverse temperature gradient. An external uniform magnetic field of intensity $\mathbf{H}$ is applied in z direction.

The main focus of this paper is the influence of the thermoelectric effect, which is acting at the interface between the liquid phase and the conducting walls. The thermoelectric effect and its consequences for magnetofluid dynamics is described in detail in a seminal paper by Shercliff [6]. Starting point is the generalized Ohm's law for an electrically conducting fluid containing an additional thermoelectric term describing the generation of the current density $\mathbf{J}$ by the temperature gradient grad T,

$$\frac{\mathbf{J}}{\sigma}=\mathbf{E}+\mu(\mathbf{u}\times\mathbf{H})-S\ \mathrm{grad}\,T. \tag{1}$$

Here σ is the electrical conductivity, $\mathbf{E}$ is the electric field, μ is the magnetic permeability, $\mathbf{u}$ is the velocity vector, S is the absolute thermoelectric power.

If the electric field is nonrotational and the thermoelectric power depends only on temperature, no thermoelectric currents arise in a homogeneous fluid, because curl$(S(T)$ grad $T)$ is zero in a homogeneous medium. This is analogous to the hydrodynamic case, where forces coming out from a scalar potential (for example, the gravitational force) are balanced by the pressure and no motion occurs. At the boundary, where S changes because of the change of material, S grad T becomes rotational, i.e. curl$(S(T)$ grad $T)\neq\mathbf{0}$ and closed currents appear at the boundary, which are determined by the *temperature distribution along the interface*. In the problem at hand the fluid rising up and coming down in consequence of convection creates hot and cool regions in the boundary layer, therethrough producing a horizontal temperature gradient on the surface fluid wall. A current flow appears parallel to the contact surface of two media with different absolute thermoelectric power (see Fig. 1). The boundary condition for the tangential components of the current density can be derived by the integration of Eq. (1) around the elementary contour covering the interface (assuming the absence of electrical field and the velocity to be zero at the interface), see Shercliff [6],

$$\frac{J_{ws}}{\sigma_w}-\frac{J_s}{\sigma_f}=P\frac{\partial T}{\partial s}. \tag{2}$$

Lower index s denotes tangential components, index f and w are used for the fluid and wall quantities appropriately, functions without index are defined for fluid. $P=S_f-S_w$ is the thermoelectric power of the metal pair.

Our aim in this section is to derive the equations for the onset of instability and the determination of the unstable modes. As it turns out the critical Rayleigh number does not depend on the influence of the thermoelectric effect, because the global system of equations describing the behavior of the Rayleigh-Bénard convection in the magnetic field between thick electrically conducting wall divides into two subsystems of equations, which are formally independent of each other, i.e., they are solved separately. The first subsystem defines the linear instability for the onset of the Rayleigh-Bénard convection and is not influenced by the thermoelectric effect (whether it is present or not). The second subsystem states how the Lorentz force of the thermoelectric currents inside the magnetic field influences the shape of the unstable mode. Therefore we first present a derivation of the first subsystem determining critical characteristics of instability in Sec. II A. In Sec. II B we investigate the second subsystem dealing with the influence of the thermoelectric effect.

A. Onset of instability

We begin now with the derivation of the first subsystem of equations, which determines the critical Rayleigh number for the instability. This result is valid *in both cases*: in the presence of the thermoelectric effect as well as without it.

Regarding buoyancy effects in the Boussinesq approximation, where the fluid is considered as incompressible except in the buoyancy force term of the Navier-Stokes equation, the fluid is described by the Navier-Stokes equation including the Lorentz force, the temperature transport equation, and the equations for the magnetic field:

$$\frac{\partial u_i}{\partial t}+u_j\frac{\partial u_i}{\partial x_j}=-\left(1+\frac{\Delta\rho}{\rho}\right)g_i-\frac{1}{\rho}\frac{\partial p}{\partial x_i}+\nu\nabla^2 u_i+\frac{\mu}{\rho}(\mathbf{J}\times\mathbf{H})_i, \tag{3}$$

$$\frac{\partial T}{\partial t}+u_j\frac{\partial T}{\partial x_j}=\kappa_f\nabla^2 T, \tag{4}$$

$$\frac{\partial H_i}{\partial t}+u_j\frac{\partial H_i}{\partial x_j}=H_j\frac{\partial u_i}{\partial x_j}+\eta_f\nabla^2 H_i, \tag{5}$$

where $i=x,y,z$. $\rho=$const is the fluid density at some properly chosen mean temperature T^* and $\Delta\rho=-\rho\alpha(T-T^*)$, where α is the coefficient of volume expansion. **g** is the acceleration due to gravity, p is pressure in the fluid, ν is the kinematic viscosity, **J** the magnetic current density. T is the temperature, κ is the coefficient of thermal diffusivity, $\eta=1/(\mu\sigma)$ is the electrical resistivity of the fluid. The magnetic field and the velocity field are solenoidal: div $\mathbf{H}=0$, div $\mathbf{u}=0$. Inside the solid walls there is no convection and one gets diffusion equations for the temperature and the magnetic field:

$$\frac{\partial T_w}{\partial t}=\kappa_w\nabla^2 T_w, \tag{6}$$

$$\frac{\partial H_{wi}}{\partial t}=\eta_w\nabla^2 H_{wi}. \tag{7}$$

The unperturbed state is characterized by quiescent fluid ($\mathbf{u}\equiv 0$) and temperature transport only by means of conduction. The solution of the temperature equations (4) with $\mathbf{u}\equiv\mathbf{0}$ in the fluid and (6) inside the walls is given by the following piecewise linear temperature profile

$$T_{w1}=T_1-\frac{\lambda_f}{\lambda_w}\beta(\delta+z), \quad -\delta<z<0, \tag{8}$$

$$T=T_1-\beta\left(\frac{\lambda_f}{\lambda_w}\delta+z\right), \quad 0<z<d, \tag{9}$$

$$T_{w2}=T_0+\frac{\lambda_f}{\lambda_w}\beta(d+\delta-z), \quad d<z<d+\delta, \tag{10}$$

where λ is the coefficient of thermal conductivity. $\beta=\tilde{\beta}(d+2\delta)/(d+2\delta\lambda_f/\lambda_w)$ is the temperature gradient, which is maintained inside the fluid. Lower index $w1$ denotes the lower wall, $w2$ the upper wall. As the temperature profile depends on the z coordinate only, there are no horizontal temperature gradients at the liquid-solid interfaces and consequently no thermoelectric currents. This means $\mathbf{J}\equiv\mathbf{0}$ in the unperturbed state.

Now we proceed with the linear stability analysis by expanding the perturbation of the initial state into normal modes. The perturbations are u,v,w for the velocity, $\theta=T-T(z)$ for the temperature, where $T(z)$ is given by Eqs. (8), (9), and (10). h_x,h_y,h_z is the deviation from the z-directed uniform magnetic field. For the vectorial quantities it is enough to consider the z components,

$$\begin{aligned} w&=W(z)\exp[i(k_x x+k_y y)+\psi t],\\ \theta&=\Theta(z)\exp[i(k_x x+k_y y)+\psi t],\\ h_z&=K(z)\exp[i(k_x x+k_y y)+\psi t], \end{aligned} \tag{11}$$

where $k=\sqrt{(k_x^2+k_y^2)}$ is the wave number of the disturbance, ψ is the growth rate of the perturbations in time. To introduce nondimensional variables we choose d as unit of length, βd as unit of temperature, d^2/ν as unit of time, H as unit of magnetic field and let $D=d(\partial/\partial z)$ and k, z be already measured in nondimensional units.

Inserting the normal mode expansions into equations (3)–(7) we get the following system of dimensionless linear equations for the marginal state (characterized by $\psi=0$):

$$(D^2-k^2)^2 W-k^2\mathrm{Ra}\Theta+(\mathcal{P}_m/\mathcal{P})^{-1}\mathrm{Ha}^2 D(D^2-k^2)K=0, \tag{12}$$

$$(D^2-k^2)\Theta+W=0, \tag{13}$$

$$(D^2-k^2)K+(\mathcal{P}_m/\mathcal{P})DW=0, \tag{14}$$

$$(D^2-k^2)\Theta_w=0, \tag{15}$$

$$(D^2-k^2)K_w=0. \tag{16}$$

The first three equations hold for the fluid and the last two equations are valid inside the walls. Here we have introduced the following nondimensional parameters: $\mathrm{Ra}=\alpha g\beta d^4/(\kappa_f\nu)$ is the Rayleigh number, $\mathrm{Ha}=d\mu H\sqrt{\sigma_f/\rho\nu}$ is the Hartmann number. The ratio of the magnetic Prandtl number $\mathcal{P}_m=\nu/\eta_f$ and the Prandtl number $\mathcal{P}=\nu/\kappa_f$ one can consider as one parameter $(\mathcal{P}_m/\mathcal{P})=\kappa_f/\eta_f$.

A solution of the Eqs. (12)–(16) must be sought that satisfies the nondimensional boundary conditions,

$$\begin{aligned} &W=0, \quad DW=0 \quad \text{for} \quad z=0 \quad \text{and} \quad z=1,\\ &\Theta_w=\Theta, \quad L_\lambda D\Theta=D\Theta_w \quad \text{for} \quad z=0 \quad \text{and} \quad z=1,\\ &\Theta_w=0 \quad \text{for} \quad z=-L_d \quad \text{and} \quad z=1+L_d, \end{aligned} \tag{17}$$

with the nondimensional parameters $L_\lambda=\lambda_f/\lambda_w$, $L_d=\delta/d$. We do not write the boundary conditions for the magnetic field because first, as it turned out, the critical Rayleigh number is determined by the Eqs. (12)–(16) with the boundary conditions (17) already selfconsistently and second we do not search the solution for the magnetic field K in the marginal stable state.

The system of Eqs. (12)–(14) can be reduced to the following differential equation for the z component of the velocity W (see Chandrasekhar [4]):

$$W^{(6)}-(3k^2+\mathrm{Ha}^2)W^{(4)}+k^2(3k^2+\mathrm{Ha}^2)W^{(2)} +k^2(\mathrm{Ra}-k^4)W=0. \tag{18}$$

The upper index in parentheses denotes the order of derivative. The general solution for W is a superposition of exponential, sine or cosine functions with unknown coefficients $C_n(n=1,\ldots,6)$ in the dependence on the roots q_n of the appropriate characteristic equation [14]:

$$q^6-(3k^2+\mathrm{Ha}^2)q^4+k^2(3k^2+\mathrm{Ha}^2)q^2+k^2(\mathrm{Ra}-k^4)=0. \tag{19}$$

These roots $q_n(n=1,\ldots,6)$ can be real or complex, simple or multiple depending on the values of $k,\mathrm{Ra},\mathrm{Ha}$. They determine the form of the function W (all possible cases are described in detail in the Appendix). Then using the Eq. (12), in which K is eliminated by help of Eq. (14), we can write the general solution for the temperature through the general solution of the velocity W in the following form:

$$\Theta=\frac{1}{k^2\mathrm{Ra}}(W^{(4)}-[2k^2+\mathrm{Ha}^2]W^{(2)}+k^4W),$$

$$\Theta_{w1}=C_7\exp[-kz]+C_8\exp[kz], \tag{20}$$

$$\Theta_{w2}=C_9\exp[-kz]+C_{10}\exp[kz],$$

where $C_7,\ldots,C_{10}$ are unknown coefficients.

To determine the ten coefficients C_n in the ansatz for the velocity W (see Appendix) and the temperature Θ (20) these expressions are inserted into the boundary conditions (17). This leads to a system of linear equations that can be written in matrix form $A\cdot\mathbf{C}=0$, where $\mathbf{C}$ denotes the vector containing the ten coefficients. The coefficients of matrix A depend on $k,\mathrm{Ra},\mathrm{Ha},L_\lambda,L_d$. A nontrivial solution exists, if $\det A=0$. This condition determines the Rayleigh number for neutral stability $\mathrm{Ra}_n=\mathrm{Ra}_n(k,\mathrm{Ha},L_\lambda,L_d)$. One gets the *critical Rayleigh number* Ra_c for the onset of convection by taking the minimum value of Ra_n in dependence on the wave number k: $\mathrm{Ra}_c(\mathrm{Ha},L_\lambda,L_d)=\min_{k\epsilon\mathbf{R}}\mathrm{Ra}_n(k,\mathrm{Ha},L_\lambda,L_d)$.

The system of equations that was considered in this section is, as already mentioned, valid both in the presence and absence of the thermoelectric effect. Therefore the value of the critical Rayleigh number is independent from the presence of the thermoelectric effect.

B. Influence of the thermoelectric effect on the unstable mode

Without regarding the thermoelectric effect the z components of the vorticity ω_z and current density J_z are zero (see [4]). The unstable solutions are convection rolls directing in an arbitrary direction of the xy plane. To take into account the consequences of the thermoelectric effect we choose the axes of the convection rolls to be parallel to the x axis (see Fig. 1, part 1). The temperature distribution in y direction shows a sinusoidal shape and creates thermoelectric currents parallel to the y axis which are strongest where the temperature curve is steepest and which are zero at the maxima and minima of the temperature distribution (see Fig. 1, part 2). The resulting Lorenz force points in the x direction, parallel to the axes of the convection rolls and its strength is an oscillating function of y (see Fig. 1, part 3).

The Lorentz force will accelerate the fluid along the axes of the convection rolls and the vorticity will additionally have a z component besides the x component. The boundary condition of the thermoelectric effect (2) for the tangential components of the current density can be transformed (using $\mathrm{div}\,\mathbf{J}=0$) into a boundary condition for J_z,

$$\frac{1}{\sigma_w}\frac{\partial J_{wz}}{\partial z}-\frac{1}{\sigma_f}\frac{\partial J_z}{\partial z}=P\left(\frac{\partial^2 T}{\partial x^2}+\frac{\partial^2 T}{\partial y^2}\right). \tag{21}$$

Thus, to describe the influence of the thermoelectric effect one needs additionally the equations for the vorticity and current density in the fluid and in the walls. We use the normal mode expansions for the z components of the perturbations of the vorticity ω_z and current density j_z:

$$\omega_z=Z(z)\exp[i(k_x x+k_y y)+\psi t],$$
$$j_z=X(z)\exp[i(k_x x+k_y y)+\psi t]. \tag{22}$$

Computing the curl of Eqs. (3), (5), and (7) and transforming to the nondimensional units we get the following system of equations for Z and X ($\psi=0$):

$$(D^2-k^2)Z+(\mathcal{P}_m/\mathcal{P})^{-1}\mathrm{Ha}^2DX=0, \tag{23}$$

$$(D^2-k^2)X+(\mathcal{P}_m/\mathcal{P})DZ=0, \tag{24}$$

$$(D^2-k^2)X_w=0. \tag{25}$$

Then the boundary conditions for the z components of the vorticity and the current density are:

$$L_\sigma DX_w-DX=K_{TE}(-k^2)\Theta,\quad X_w=X\quad \text{for}$$
$$z=0\quad\text{and}\quad z=1,$$
$$X_w=0\quad\text{for}\quad z=-L_d\quad\text{and}\quad z=1+L_d, \tag{26}$$
$$Z=0\quad\text{for}\quad z=0\quad\text{and}\quad z=1.$$

Here two new nondimensional parameters appear: $L_\sigma=\sigma_f/\sigma_w$ and the thermoelectric parameter $K_{TE}=P\beta d\sigma_f/H$. The first boundary condition in Eqs. (26) is the condition of the thermoelectric effect (21) now in dimensionless form.

We remind that the system (23)–(25) describing the influence of the thermoelectric effect is formally independent from the system (12)–(16) describing the onset of instability. The system (23)–(25) is added to the system (12)–(16), if the thermoelectric effect must be taken into account. It can be once more pointed out that on the ground of the indepen-

dence of these two systems the critical Rayleigh number comes only from the system (12)–(16), even though the thermoelectric effect is present.

Eliminating the vorticity one receives one differential equation for the current density in the fluid

$$X^{(4)}-(2k^2+\mathrm{Ha}^2)X^{(2)}+k^4X=0. \tag{27}$$

The characteristic equation of this equation has only real roots $\varphi_1,\ldots,\varphi_4$. Equation in the walls (25) is solved separately and the general solution for current density is given as

$$X=\sum_{n=1}^{4} G_n\exp[\varphi_n z],$$

$$X_{w1}=G_5\exp[kz]+G_6\exp[-kz], \tag{28}$$

$$X_{w2}=G_7\exp[kz]+G_8\exp[-kz].$$

Here $G_1,\ldots,G_8$ are unknown coefficients. If the solution for the current density X is known, then the solution for the vorticity Z is gained by integration of Eq. (24). Substituting this expression for the vorticity Z in Eq. (23) we find that the constant of integration is equal to zero. Then the general solution for the vorticity is

$$Z=-(\mathcal{P}_m/\mathcal{P})^{-1}\sum_{n=1}^{4} G_n\frac{\varphi_n^2-k^2}{\varphi_n}\exp[\varphi_n z]. \tag{29}$$

The general solutions for Z and X being inserted in the boundary conditions (26) give an inhomogeneous system of linear equations for determination of the G_n. This system can be written in matrix form as $M\cdot\mathbf{G}=\mathbf{F}$, where the elements of matrix M and right-hand side vector $\mathbf{G}$ are given.

Thus we have surveyed the solution of the systems (12)–(16) and (23)–(25) from five and three differential equations with the boundary conditions (17) and (26) accordingly, which in total contain the seven nondimensional parameters: $\mathrm{Ra},\mathrm{Ha},(\mathcal{P}_m/\mathcal{P}),L_\lambda,L_d,L_\sigma,K_{TE}$, described above.

III. NUMERICAL ANALYSIS AND RESULTS

In Sec. II we derived the matrix equations for the coefficients of the general solution first for the determination of the critical Rayleigh number and second for the determining how the unstable mode is changed by the thermoelectric effect. These equations are solved numerically with help of the LU decomposition method [15]. This section is divided into two subsections. The first one deals with the determination of the critical Rayleigh number and the second one with the thermoelectric effect.

A. Computation of the critical Rayleigh number

As it is already stated in Sec. II A $\mathrm{Ra}_c=\mathrm{Ra}_c(\mathrm{Ha},L_\lambda,L_d)$. The ratio L_λ between the thermal conductivities of the fluid and wall and the ratio L_d of the fluid and wall thickness' come into the problem because the thick walls are considered. To show the influence of the thick walls on the critical Rayleigh number we present in Figs. 2(a) and 2(b) the Ra_c and the corresponding wave number k_c as a functions of L_d. Two curves for $\mathrm{Ha}=0$ and $\mathrm{Ha}=1$ are shown, the ratio L_λ is fixed to 0.5. Increasing of the Hartmann number leads to an increase of the critical Rayleigh number, because magnetic field has the tendency to suppress convection. In absence of the conducting walls — corresponding to $L_d=0$ — the obtained results can be compared with the computation data of Chandrasekhar [4] in case of the both rigid boundaries (see Table I).

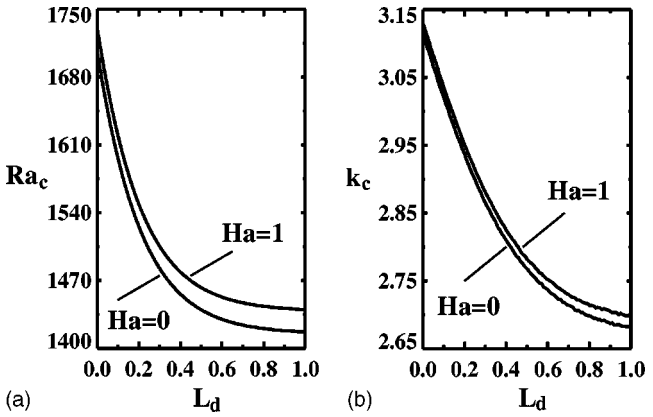

FIG. 2. Critical Rayleigh number (a) and wave number (b) as a functions of the parameter L_d (the ratio between fluid layer and wall thickness') for $\mathrm{Ha}=0$ and $\mathrm{Ha}=1$ at $L_\lambda=0.5$ in the state of the stationary convection.

From Fig. 2(a) we observe a destabilizing influence of the conducting walls compared to $L_d=0$ on the stability state. This means if the thickness of the walls increases (L_d increases) then instability occurs at a lower value of the critical Rayleigh number. This can be explained by the nature of the physical processes taking place in the Rayleigh-Bénard convection. As known (for example, from the detailed description of convection given by Normand *et al.* [16]) the vertical temperature gradient maintained in the fluid has the consequence that there is light fluid below heavy fluid because of thermal expansion. Accordingly the parts of the fluid have a natural tendency to redistribute themselves in order to amend the formed disbalance. Instability occurs at minimum temperature gradient at which the stabilizing effect of viscosity and thermodiffusion are overcome by the destabilizing buoyancy. In presence of the conducting walls there appears the boundary condition (17) of a constancy of the heat current through boundary interface between the wall and fluid. This heat current in z direction from bottom wall to fluid is addi-

TABLE I. Comparison of the critical Rayleigh numbers and the wave numbers, computed on the base of present theory (at equality to zero of the wall thickness) with the result of Chandrasekhar [4] (both bounding surfaces are rigid).

	Numerical computation of present theory		The Chandrasekhar's results	
Ha	k_c	Ra_c	k_c	Ra_c
0	3.11	1707.768	3.13	1707.8
10	4.01	3757.229	4	3757.3

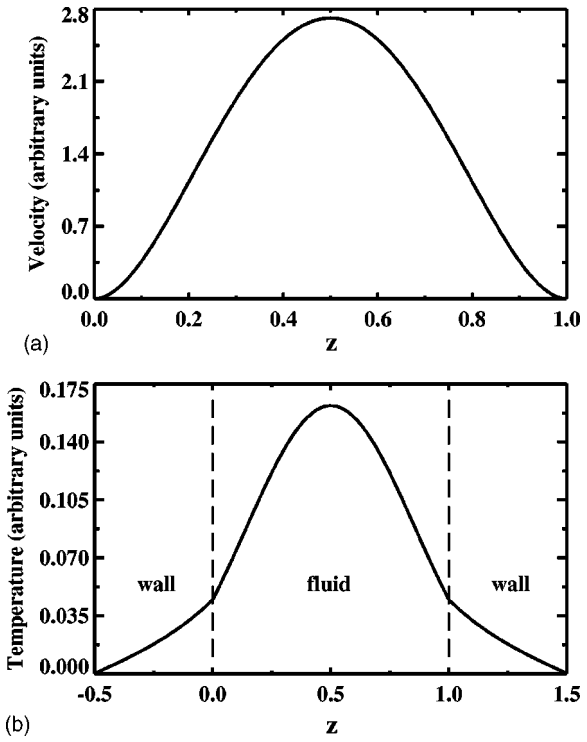

FIG. 3. The solution for the z components of the velocity W (a) and of the temperature Θ in the fluid and walls (b) for the state of the marginal stability at $\mathrm{Ha}=1, L_\lambda=0.5, L_d=0.5$.

tional driving force of the convection. Whereas temperature gradient in fluid and forces inhibiting the convection (viscosity and thermodiffusion) are the same as previously. Therefore the instability can manifest itself already at a lower adverse temperature gradient, i.e., at a lower value of the Rayleigh number.

The z components of the velocity W and temperature Θ for the mode of neutral stability at $\mathrm{Ha}=1, L_\lambda=0.5, L_d=0.5$ (with the coefficient C_{10} in Eq. (20) set equal to 1) is plotted in Figs. 3(a) and 3(b). Only the z dependence is shown, in horizontal direction (normal to axis of the convection rolls) the velocity and temperature are oscillating functions with wavelength $L_c=2\pi/k_c$. In the graphic 3(b) for the temperature Θ one can see a kink of the curve at transition across the wall-fluid interface. The temperatures of the wall and fluid in kink point are equal, but the derivatives of the temperature functions are different in the wall and fluid. The slope of the temperature curve changes at interface, because wall and fluid have different thermal conductivities.

At the end of this section we enter an additional verification of received results for the marginal stability curves in the two limit cases of the parameter L_d, namely, $L_d\to 0$ and $L_d\to\infty$. The limits of the critical Rayleigh number in these limit cases we will name Ra_{c0} and $\mathrm{Ra}_{c\infty}$ appropriately. In both limit cases the matrix A, with help of which the critical Rayleigh number is determined, can be simplified.

First we have made numerical calculations in the frame of an analysis where the wall thickness δ is assumed to be small in comparison with the fluid layer thickness $d(\delta\ll d\Leftrightarrow L_d\ll 1)$. In this case one can approximate the temperature in the

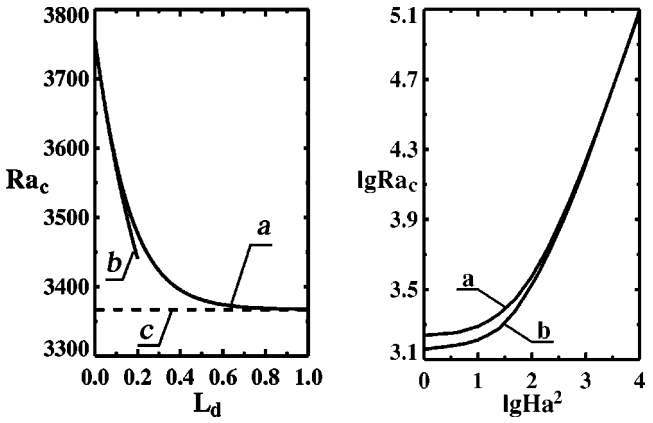

FIG. 4. (a) Critical Rayleigh number as a function of L_d (the ratio between fluid layer and wall thickness') at $\mathrm{Ha}=10, L_\lambda=0.5$: curve a is gained using the full system of equations, curve b for the case when the wall thickness is considered as small in comparison with the fluid layer thickness $L_d\ll 1$ (the temperature function in the walls behaves as a linear function). Curve c presents the asymptotic behavior of the critical Rayleigh number at $L_d\to\infty$ (the temperature in the walls can be described by one exponential function). (b) Dependence of the limits of the critical Rayleigh number at $L_d\to 0$ and $L_d\to\infty$ on the Hartmann number, curve a presents Ra_{c0} and curve b $\mathrm{Ra}_{c\infty}$.

walls by a linear function of the z coordinate

$$\Theta_{w1}=C_7'+C_8'z,$$

$$\Theta_{w2}=C_9'+C_{10}'z,$$

because the partial derivatives in x and y direction are much smaller than the partial derivative in z direction. Figure 4(a) represents again the critical Rayleigh number as a function of L_d. Curve a is computed using the full heat equation and curve b is computed by the linear approximation for thin walls. In the interval $0<L_d<0.1$ both curves are in good agreement, but for higher values of L_d the linear approximation is no longer appropriate and the destabilizing effect of the heat conducting walls is overestimated.

Second we explore the marginal stability state in case of the high limit of L_d, when the fluid layer thickness d is much smaller than the wall thickness δ $(d\ll\delta\Leftrightarrow L_d\gg 1)$. Then limit evaluation at $L_d\to\infty$ in the boundary conditions (17) gives the possibility to describe the temperature functions in the walls as depending only on one exponential function,

$$\Theta_{w1}=C_8''\exp[kz],$$

$$\Theta_{w2}=C_9''\exp[-kz].$$

Accordingly this procedure decreases linear size of the matrix A by 2. The reduced matrix A does not depend on the parameter L_d and one can numerically compute the asymptote, to which the critical Rayleigh number approaches at $L_d\to\infty$. This asymptote $\mathrm{Ra}_{c\infty}=3367.010\,99$ labeled c is dashed in Fig. 4(a). In the computation shown in Fig. 4(a) we have chosen a higher value of the Hartmann number $\mathrm{Ha}=10$ in order to enhance the influence of the magnetic field

(L_λ still is 0.5). The critical Rayleigh number is more than twice the value as in Fig. 2(a) for Ha=0 and Ha=1, which demonstrates the stabilizing effect of the magnetic field.

The dependence of the critical Rayleigh number on the parameter L_d can be approximated by the exponential function as

$$\mathrm{Ra}_c = \mathrm{Ra}_{c\infty} + \exp[-kL_d],$$

where, for example, for Ha=10 and $L_\lambda = 0.5$ [as in Fig. 4(a)] the exponent is found to be close to $k \approx 7$.

In Fig. 4(b) we present a dependence of the both limits of the critical Rayleigh number Ra_{c0} and $\mathrm{Ra}_{c\infty}$ on the Hartmann number up to Ha=100.

B. Measures of the influence of the thermoelectric effect

We have already found out that the thermoelectric effect does not change the critical Rayleigh number for onset of convection. In this section we shall answer the question: how is the unstable mode influenced by the thermoelectric effect? Additionally we define two quantities that are suitable to show the strength of the influence of the thermoelectric effect.

The thermoelectrical parameter K_{TE} is present only in the boundary conditions (26) for the z components of the vorticity Z and the current density X. Namely the right-hand side vector $\mathbf{F}$ of the system $M \cdot \mathbf{G} = \mathbf{F}$ for determination of $G_n (n = 1, \ldots, 8)$ includes K_{TE}. As the result of numerical solution of this system Figs. 5(a) and 5(b) illustrate the behavior of Z and X in the marginal stable state for Ha=1, $L_\lambda = 0.5, L_d = 0.5$ (the same parameters as for Fig. 3), $(\mathcal{P}_m/\mathcal{P}) = 0.5 \times 10^{-5}, L_\sigma = 0.5$. Given results were computed at the thermoelectrical parameter $K_{TE} = 0.1$. As for W and Θ in Fig. 3 also for Z and X arbitrary units are used, because the linear equations for the unstable mode give only a linear subspace as a solution.

To clear up the influence of the thermoelectric effect on the shape of the unstable mode we search the horizontal components of the velocity u, v and vorticity ω_x, ω_y. From the substitution (11) we get the z components of the velocity w and vorticity ω_z. Then we find u, v from system,

$$\frac{\partial u}{\partial x} + \frac{\partial v}{\partial y} = -\frac{\partial w}{\partial z},$$

$$\frac{\partial v}{\partial x} - \frac{\partial u}{\partial y} = \omega_z,$$

and ω_x, ω_y as follows,

$$\omega_x = \frac{\partial w}{\partial y} - \frac{\partial v}{\partial z},$$

$$\omega_y = \frac{\partial u}{\partial z} - \frac{\partial w}{\partial x}. \tag{30}$$

The z component of the vorticity ω_z is function of the K_{TE} number, which enters into the boundary conditions (26). Therefore the general vectors of the velocity $\mathbf{u} = (u, v, w)$ and vorticity $\boldsymbol{\omega} = (\omega_x, \omega_y, \omega_z)$ are also functions of the K_{TE}. Thus the thermoelectrical effect being induced by the convection influences itself the convection by changing the shape of the unstable mode, whereas the critical Rayleigh number remains unchanged. The qualitative three-dimensional schema of the fluid convection flow in the state of the marginal stability is sketched in Fig. 6, from which one can see that the streamlines inside of a convection roll are situated in vertical planes. Though under the influence of the thermoelectric effect these planes are turned around a vertical axis by an angle γ [see also Fig. 8(a)]. This angle is determined by amount of the K_{TE} number. We define angle γ for the marginal stability state as follows:

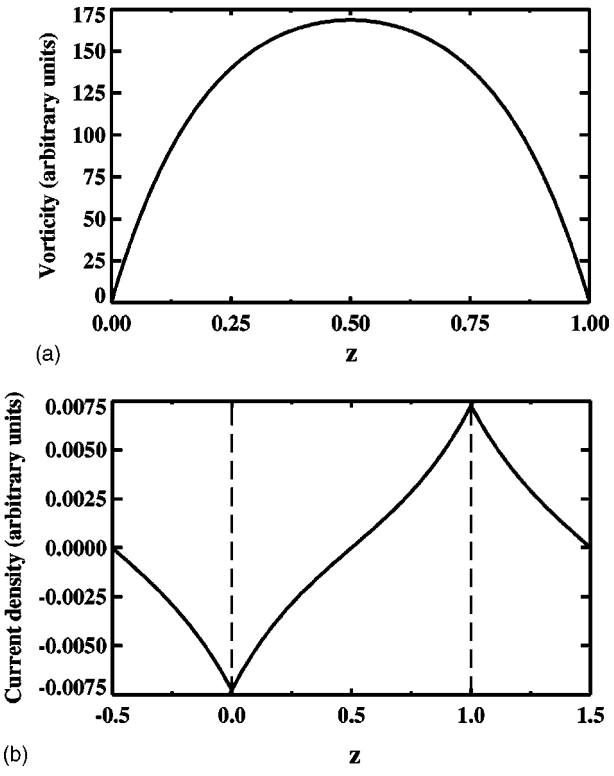

FIG. 5. The solution for the vorticity Z (a) and for the current density X in the fluid and walls (b) for the state of the marginal stability at Ha=1, $L_\lambda = 0.5, L_d = 0.5, (\mathcal{P}_m/\mathcal{P}) = 0.5 \times 10^{-5}, L_\sigma = 0.5, K_{TE} = 0.1$.

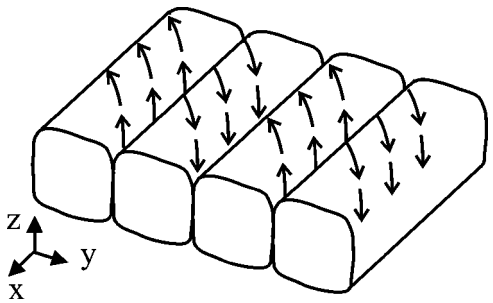

FIG. 6. The qualitative three-dimensional schema of the convection rolls position influenced by the thermoelectric effect in the state of the marginal stability.

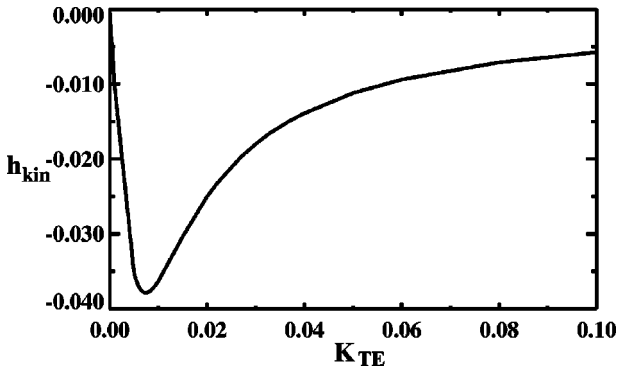

FIG. 7. Kinetic helicity as a function of the thermoelectric parameter K_{TE} in the state of the marginal stability at Ha$=1$,$L_d=0.5$,$L_\lambda=0.5$,$L_\sigma=0.5$,$(\mathcal{P}_m/\mathcal{P})=0.5\times10^{-5}$.

$$\gamma=\lim_{z\to 0}\left|\arctan\frac{u(z)}{v(z)}\right|. \tag{31}$$

For the fluid and walls in the given system a concrete metal pair can be taken. Then the angle γ will depend on the parameters $L_\lambda, L_\sigma, (\mathcal{P}_m/\mathcal{P})$ characterizing the properties of metals, and on Ha,L_d. The angle γ will magnify with growing parameter K_{TE}. This fact can be also represented by behavior of the relative kinetic helicity

$$h_{kin}=\frac{\int\int_\Omega\int \mathbf{u}\cdot\boldsymbol{\omega}\,dx\,dy\,dz}{\sqrt{\int\int_\Omega\int \mathbf{u}^2\,dx\,dy\,dz\int\int_\Omega\int \boldsymbol{\omega}^2\,dx\,dy\,dz}},$$

(where Ω is volume of integration) as a function of the K_{TE} number (see Fig. 7) at Ha$=1$,$L_d=0.5$,$L_\lambda=0.5$,$L_\sigma=0.5$,$(\mathcal{P}_m/\mathcal{P})=0.5\times10^{-5}$.

Thus we can close about a physical treatment of the the influence of the thermoelectric effect following. The current flow arising in fluid-wall boundary layer as result of the horizontal temperature gradient on this interface creates the Lorentz force that is parallel to the boundary surface and parallel to the convection rolls axis. However, the Lorentz force has different absolute value along of the *y* direction. It leads to a helical flow inside the convection rolls.

IV. CONCLUSION

In summary, we want to conclude that the thermally and electrically conducting walls have destabilizing influence upon the stability set in the Rayleigh-Bénard problem inside the magnetic field. The thermoelectric effect (taken into account as the boundary condition on the fluid-wall interface) does not affect the critical Rayleigh number, but changes the shape of unstable mode.

The prediction of the influence of the thermoelectric effect upon the shape of unstable modes of the solid-liquid system Al-Li can be instanced qua numerical test. For given metal pair the angle γ of the convection rolls deviation is the increasing function of the K_{TE} number, graph of which is plotted in Fig. 8(b). This function of the dependence of the

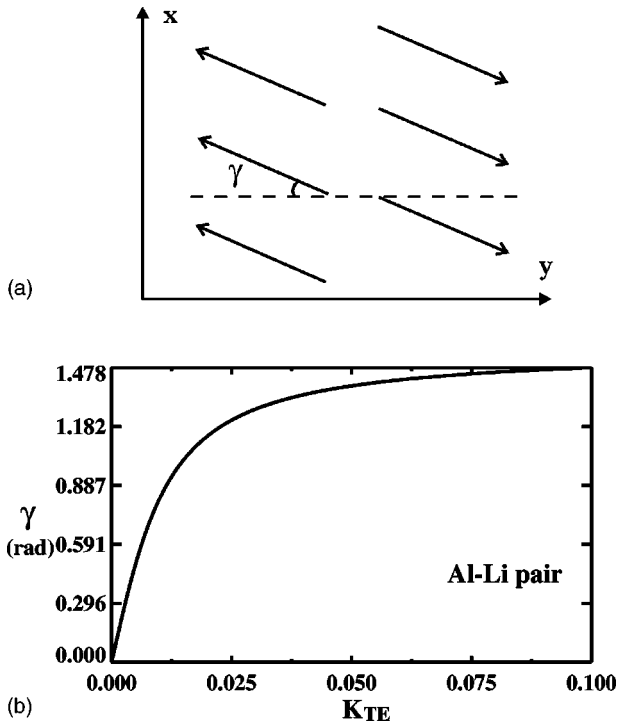

FIG. 8. The angle γ of the convection rolls deviation under influence of the thermoelectric effect in the state of the marginal stability (the schematic view from above) (a); the angle γ as a function of the thermoelectrical parameter K_{TE}, calculated for the Al-Li solid-liquid system at Ra$=1462.64$,Ha$=1$,$L_d=0.5$ (b).

angleγ on K_{TE} is computed at Ra$=1462.64$, Ha$=1$, $L_d=0.5$ with help of the formula (31).

The parameter $K_{TE}=(P\beta d\sigma_f)/H$ is determined by the thermoelectric power P of the metal pair, electrical conductivity of the liquid phase σ_f, maintained temperature gradient β in the fluid, thickness d of the liquid layer, and intensity H of the magnetic field. For the Al-Li pair $P\approx30$ (μV/K) [6], $\sigma_f=\sigma_{Li}$. There are three further parameters β, d, and H, which are independent on the properties of chosen metals. But to calculate the K_{TE} number and the corresponding angle γ for the Al-Li pair one can not freely give a numerical values for all three coefficients β, d, and H, because these coefficients are interrelated by Ra and Ha numbers. We can preset an arbitrary numerical value only for one from the coefficients β, d or H. Then we can calculate the other two coefficients from the following relations:

$$\beta d^4=\text{const}_1,$$

$$dH=\text{const}_2. \tag{32}$$

Here const_1 and const_2 are specified by concrete metals and by the fixed Ra and Ha numbers, at which the given angle γ as function from K_{TE} was computed. For example, for the solid-liquid system Al-Li at magnetic field $\mathbf{B}=1$ mT we get from Eq. (32) $d=16.1$ mm, $\beta=208{,}255$ (K/m). Upon that the parameter $K_{TE}\approx0.022\,20$, it adds up to the angle $\gamma\approx67.31°$.

We note also that in absence of the thermoelectric effect the $\lim_{K_{TE}\to 0}\gamma=0$, i.e., the convection rolls do not deviate from the zy plane; with growth of the thermoelectric effect the turn of the rolls increases with increasing value of K_{TE}. For $K_{TE}\to\infty$ the angle γ approches $\pi/2$ asymptotically. The value of $\pi/2$ is of couse never reached for finite value of K_{TE}.

ACKNOWLEDGMENTS

We are grateful to the DLR (Deutsches Zentrum für Luft- und Raumfahrt) for financial support and to T. Boeck and W. Boos for helpful discussions. We thank Y. Ponty for his advice to explore the limit $L_d \gg 1$.

APPENDIX

In the Appendix we present the forms of solution of the differential equation (18) for velocity W in dependence on the k, Ra, Ha. These forms of solution are necessary to insert them in the solution for temperature (20) and in the boundary condition (17).

The general solution for W can be written as superposition

$$W=C_1f_1(z)+C_2f_2(z)+C_3f_3(z)+C_4f_4(z)+C_5f_5(z)+C_6f_6(z). \tag{A1}$$

Here $C_i\,(i=1,\ldots,6)$ are unknown coefficients, the functions $f_i\,(i=1,\ldots,6)$ are determined by the six roots of the characteristic equation (19). The characteristic equation (19) is reduced by the substitution

$$q^2=\chi \tag{A2}$$

to the cubic equation

$$\chi^3+a_2\chi^2+a_1\chi+a_0=0, \tag{A3}$$

where $a_0=k^2(\mathrm{Ra}-k^4)$, $a_1=k^2(3k^2+\mathrm{Ha}^2)$, $a_2=-(3k^2+\mathrm{Ha}^2)$. Define the parameter A and B as follows:

$$A=\frac{1}{3}a_1-\frac{1}{9}a_2^2,\qquad B=\frac{1}{6}(a_1a_2-3a_0)-\frac{1}{27}a_2^3. \tag{A4}$$

The sign of quantity A^3+B^2 determines whether the roots of characteristic equation (A3) are real (different or multiple) or complex. Three cases ($A^3+B^2>0,<0$ or $=0$) specify appropriately the form of solution of the Eq. (18).

One of the roots of the Eq. (A3) χ_1 is always real irrespective of the sign of quantity A^3+B^2. It is of importance this root χ_1 is positive, negative or equal to zero. If $\chi_1>0$ then two real roots q_1 and $q_2=-q_1$ found from Eq. (A2) yield the functions (see also [14])

$$f_1(z)=\exp[q_1z],\qquad f_2(z)=\exp[q_2z]. \tag{A5}$$

If $\chi_1<0$ then it is found from Eq. (A2) two complex conjugate roots q_1,q_2 with only imaginary parts. Corresponding functions f_1,f_2 are

$$f_1(z)=\cos[\mathrm{Im}(q_1)z],\qquad f_2(z)=\sin[\mathrm{Im}(q_2)z]. \tag{A6}$$

In the case $\chi_1=0$ we have two-multiple root $q_1=q_2=0$ and

$$f_1(z)=1,\qquad f_2(z)=z. \tag{A7}$$

Thereby all possibilities for f_1,f_2 are over. Consider remaining four function $f_i\,(i=3,\ldots,6)$.

(1) If $A^3+B^2>0$ then the Eq. (A3) has besides one real root χ_1 another two complex conjugate roots χ_2,χ_3. Thus using (A2) we get another four roots for the equation (19). They are two pairs of the complex conjugate roots q_3,q_4 and $q_5=-q_3$, $q_6=-q_4$. In this case the functions $f_i\,(i=3,\ldots,6)$ have the form

$$\begin{aligned} f_3&=\exp[\mathrm{Re}(q_3)z]\cos[\mathrm{Im}(q_3)z],\\ f_4&=\exp[\mathrm{Re}(q_4)z]\sin[\mathrm{Im}(q_4)z],\\ f_5&=\exp[\mathrm{Re}(q_5)z]\cos[\mathrm{Im}(q_5)z],s\\ f_6&=\exp[\mathrm{Re}(q_6)z]\sin[\mathrm{Im}(q_6)z]. \end{aligned} \tag{A8}$$

(2) If $A^3+B^2<0$ then the Eq. (A3) has besides one real root χ_1 another two real roots χ_2 and χ_3. Upon that all three roots are different. In this case signs of χ_2 and χ_3 determine via Eq. (A2) the roots q_i and form of $f_i\,(i=3,\ldots,6)$. If $\chi_2>0$ then

$$f_3(z)=\exp[q_3z],\qquad f_4(z)=\exp[q_4z]. \tag{A9}$$

If $\chi_2<0$ then

$$f_3(z)=\cos[\mathrm{Im}(q_3)z],\qquad f_4(z)=\sin[\mathrm{Im}(q_4)z]. \tag{A10}$$

If $\chi_2=0$ then

$$f_3(z)=1,\qquad f_4(z)=z. \tag{A11}$$

Analogically one can write the function f_5,f_6 for $\chi_3>0,\chi_3<0,\chi_3=0$, counting that χ_1,χ_2,χ_3 can not be equal to zero simultaneously.

(3) If $A^3+B^2=0$ ($A^3=-B^2\neq 0$) then the equation (A3) has two equal roots $\chi_2=\chi_3$. With that if $\chi_2=\chi_3>0$ then $q_3=q_4>0$, $q_5=q_6=-q_3<0$ and

$$f_3(z)=\exp[q_3 z],$$
$$f_4(z)=z\exp[q_4 z],$$
$$f_5(z)=\exp[q_5 z],$$
$$f_6(z)=z\exp[q_6 z]. \tag{A12}$$

If $\chi_2=\chi_3<0$ then

$$f_3(z)=\cos[\mathrm{Im}(q_3)z],$$
$$f_4(z)=z\cos[\mathrm{Im}(q_3)z],$$
$$f_5(z)=\sin[\mathrm{Im}(q_5)z],$$
$$f_6(z)=z\sin[\mathrm{Im}(q_5)z]. \tag{A13}$$

If $\chi_2=\chi_3=0$ then

$$f_3(z)=1,$$
$$f_4(z)=z,$$
$$f_5(z)=z^2,$$
$$f_6(z)=z^3. \tag{A14}$$

If $A^3+B^2=0$ $(A=B=0)$ then solution of function W has polynomial form

$$W=(C_1+C_2z+C_3z^2)\exp[q_1z]+(C_4+C_5z+C_6z^2)\exp[q_2z], \tag{A15}$$

where $q_1=\sqrt{\chi_1}$, $q_2=-\sqrt{\chi_1}=-q_1$.

[1] Y. Nakagava, Nature (London) **175**, 417 (1955).
[2] Y. Nakagava, Proc. R. Soc. London, Ser. A **240**, 108 (1957).
[3] Y. Nakagava, Proc. R. Soc. London, Ser. A **249**, 138 (1959).
[4] S. Chandrasekhar, *Hydrodynamic and Hydromagnetic Stability* (Dover Publications, New York, 1961).
[5] R. Moreau, *Magnetohydrodynamics* (Kluwer Academic Publishers, Dordrecht, 1990).
[6] J.A. Shercliff, J. Fluid Mech. **91**, 231 (1979).
[7] O. Lielausis *et al.*, in International Symposium on Electromagnetic Processing of Materials, Tokyo, Japan, 1994, edited by The Iron and Steel Institute of Japan.
[8] P. Lehmann *et al.*, Mater. Sci. Forum **217-222**, 235 (1996).
[9] P. Lehmann *et al.*, in *Progress in Fluid Flow Research: Turbulence and Applied MHD* (American Institute of Aeronautics and Astronautics, Reston, 1998), V. 182.
[10] R. Moreau, O. Laskar, and M. Tanaka, in International Symposium on Electromagnetic Processing of Materials (Ref. [7]).
[11] Y.Y. Khine and J.S. Walker, in Proceedings of the First Hydromag Conference PAMIR, Aussois, France, 1997.
[12] G. Müller, A. Ostrogorsky, in *Handbook of Crystal Growth*, edited by D.T.J.Hurle, (Elsevier Science, Amsterdam, 1994), Vol. 2.
[13] D.T.J. Hurle and R.W. Series, in *Handbook of Crystal Growth* (Ref. [12]).
[14] I.N. Bronstein *et al.*, *Taschenbuch der Mathematik*, 4th ed. (Verlag Harry Deutsch, Frankfurt am Main, 1999).
[15] W.H. Press *et al.*, *Numerical Recipes* (Cambrige University Press, Cambridge, 1986).
[16] C. Normand, Y. Pomeau, and M.G. Velarde, Rev. Mod. Phys. **49**, 591 (1977).